Title
PLASMA AND OPERATIONAL CONDITIONS IN A HIGH SPECIES FILTER BUCKET SOURCE

Authors
Pincosy, P.A.
Ehlers, K.W.
Lietzke, A.F.

Publication Date
1986

LBL-17732
Preprint

Lawrence Berkeley Laboratory
UNIVERSITY OF CALIFORNIA

Accelerator & Fusion
Research Division

Submitted to Review of Scientific Instruments

PLASMA AND OPERATIONAL CONDITIONS IN A HIGH SPECIES FILTER BUCKET SOURCE

P.A. Pincosy, K.W. Ehlers, and A.F. Lietzke

January 1986

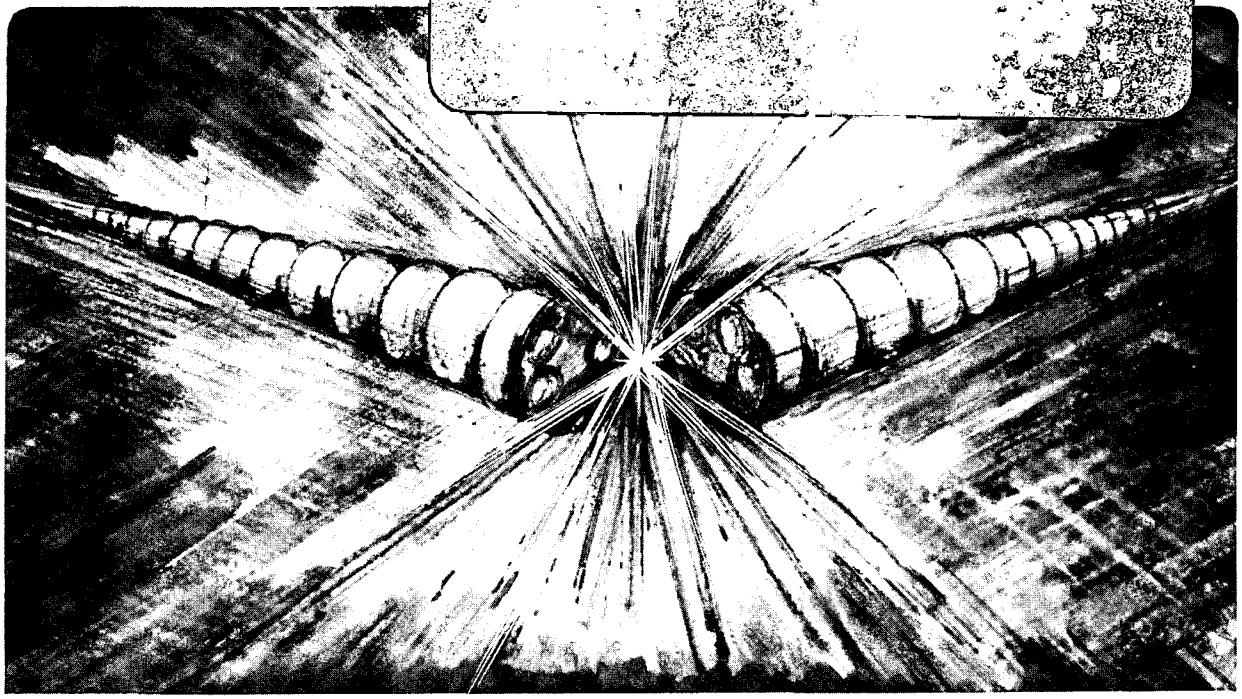

Prepared for the U.S. Department of Energy under Contract DE-AC03-76SF00098

DISCLAIMER

PLASMA AND OPERATIONAL CONDITIONS IN A HIGH SPECIES FILTER BUCKET SOURCE*

P. A. Pincosy, K. W. Ehlers and A. F. Lietzke

Lawrence Berkeley Laboratory
University of California
Berkeley, CA 94720

ABSTRACT

Experimental details of operation and plasma flow are presented for bucket ion sources having magnetic flux that bridges the source between the regions of electron injection and ion extraction. The basic goal is to increase the atomic fraction of hydrogen and deuterium by 15% and yet retain an ion flux density uniformity over the extraction region to within ± 7%. A rod structure containing permanent magnets produces a known bridging flux across a well defined region. This provides an experimental apparatus useful for the study of the effect of magnetic flux on the source plasma flow. The parameters of filter position, filter strength, filter orientation, arc power, and gas pressure are related to species fractions, profile uniformity, and electrical efficiency.

The option of having the bridging flux without a rod structure is presented and experimental results of sources thought to contain this field configuration are discussed.

*This work was supported by DOE under contract number DE-AC03-76SF00098.

INTRODUCTION

Throughout the development of ion sources for neutral beam systems, the atomic fraction any particular source configuration might produce could not be accurately predicted. Typically, [1-4] the percentage of H^+ (D^+) is between 60 and 80%, but some sources have produced higher values.[5,6] Of all the production and loss mechanisms which occur in an arc discharge geometry, it has been difficult to optimize the parameters resulting in the highest atomic fraction at the extraction grid. A number of recent experimental sources[7-9] have identified an essential feature which will definitely produce a higher atomic fraction. Ehlers and Leung[7,8] have shown that magnetic flux separating the region of electron injection from the region of ion extraction, results in an increased atomic fraction. Details of production and loss mechanisms are not sufficiently well known to give a complete understanding of the role of the magnetic filter. However, its purpose, to prevent primary, ionizing electrons from reaching the extraction region is achieved by applying a magnetic flux barrier which contains the primary electrons in the injection region. Thus only cold electrons are present in the extraction chamber. Only the H_2^+ (D_2^+) ions that survive the drift through this chamber are available for acceleration. A magnetic filter applied to the LBL 10 x 10 cm^2 bucket source[10] has resulted in an increase of the atomic fraction.[9] The data being presented reinforces the trends shown by Ehlers and Leung and gives more details of the plasma properties as well as additional operational details about the source elements.

Producing a uniform plasma density at the beam forming electrode is difficult for any large area ion source. Magnetic fields adversely

affect[11] the uniformity of ion flux density. One experiment using the filterless source indicates that magnetic flux across the source can improve the atomic fraction, but also tends to decrease the uniformity. Some evidence is given to show that the transverse fields affect the plasma density profile through the cross-field motion of the ions and electrons.

The addition of the magnetic filter structure to a magnetic bucket source, also reduces the power efficiency. The relationship between efficiency and the filter field strength and the filter position is presented.

The principal concern for an internal filter structure is the power deposited by the backstreaming electrons onto the tube structure that contains filter magnets. For the slot accelerator used,[13] calorimetry data is presented showing the integrity of the filter structure in the source and beam environment. Data taken using another source designed so that magnetic flux bridges the filaments without the use of an internal structure indicates that it may be possible to build a filter source[12] without an internal filter structure.

I. EXPERIMENTAL APPARATUS

An LBL 10 x 10 cm^2 extraction area bucket source[10] was fitted with a planar array of access holes permitting the installation of four 8mn diameter copper tubes across the plasma chamber (Fig. 1). One set of holes was in a plane at 9.5 cm from the extraction plane and a second set permitted a filter plane at 5.5 cm (not shown). Each tube contained a row of 4.8 mm square permanent magnets: either a ceramic type ("weak":

about 1500 gauss face field), or samarium cobalt ("strong": about 3000 gauss face field). This provided two filter strengths for testing. The magnetic tubes divided the plasma chamber into two sections: the section in the rear where the filaments are located, we called the source chamber or injection region, and the one where the ions are extracted, we called the extraction region.

Langmuir probes, a momentum analyzer, and electrical monitors were used to diagnose the operation. Probes were placed at a variety of locations to measure electron temperature, plasma potential, floating potential, and the ion flux density. The momentum analyzer was positioned to extract ions from the center of the source extraction region and was biased ~ 50 volts below anode potential. Arc current and voltage were monitored, as was the extraction grid potential (normally floating). These signals were measured to determine the source efficiency, "mode" of arc discharge operation, and the ionic composition. The four magnet tubes could be rotated to produce either an alternating line-cusp field (like that employed on the bucket walls) or a transverse linking field (where the flux tranverses the bucket without reversing direction). The magnetic field variation along the axis midway between two rods is shown in Figure 2 for both orientations. The total flux for the two orientations is about the same but is more concentrated in the transverse orientation. At the same time the transverse orientation has a return flux which is spread over an unspecied region. The transverse integrated flux is 180 gauss-on (SmCo) or ~90 gauss-cm (ceramic).

II. SOURCE CHARACTERISTICS

A. Stability

This source, without the magnetic filter,[10] has a discharge mode which results in inefficient plasma production. This mode occurs when the injected electron current drives the plasma potential in the source negative with respect to the anode.[14] A sheath forms at the anode with a voltage drop to the potential of the plasma which adjusts itself with respect to the anode so that electrons injected from the filament balance those lost to the anode. The presence of this mode is best indicated by the extraction grid floating potential when it falls closer to cathode potential. This operating mode can occur in a plasma notch (brief decrease of arc power) for beam turn-on, making high voltage turn-on difficult. With the addition of the magnet filter structure enough anode was added to eliminate this mode of operation.

B. GRID POTENTIAL

Without the filter, the floating potential of the extraction grid is normally between 40 and 60% of anode potential. As shown in Fig. 3, this depends crucially upon the pressure in the source. If a significant high energy tail is eliminated from the electron energy distribution, the floating potential will be within a few electron temperatures of plasma potential. The stronger filter (Figure 3) results in a more positive floating potential, since some energetic electrons can penetrate the weaker filter via collisions in the pressure range of 4 to 8 mT. For deuterium operation with the weak filter the floating potential is increased from -35 ±5 volts with no filter up to -15 ±5 volts. The

strong filter further reduces the floating potentials to between -3 and -6 volts. In this case a Langmuir probe at the extraction grid indicates a maxwellian straight line distribution (see Figure 6b) over three orders of magnitude. For a maxwellian distribution the floating potential[15] relative to the plasma potential can be calculated from the measured temperature.

$$V_f = -\frac{kT_e}{2} \ln \left(2.718 \frac{M}{2\pi m}\right) \simeq 3.7\ kT_e \qquad (1)$$

M and m are the ion and electron mass, respectively. When the strong filter source operated at 5.5 mT and with 30 kW of arc power, the measured electron temperature was 1.9 eV and the plasma potential was 3.5 volts above anode. Using the above relationship, V_f is calculated to be 7 volts below the plasma potential or 3.5 volts negative of anode potential. This value compares well with the grid floating potential measured at 3.2 volts below anode. For the weak filter at 3.7 mT source pressure shown in Figure 3, the floating potential was measured at 17 volts below anode. From the measured electron temperature of 4.3 eV and plasma potential of 1.4 eV, the calculated floating potential should have been 12.8 volts below anode. Since the electron energy distribution is not completely maxwellian and since some energetic electrons have been found to penetrate the filter into the extraction region[9] this disagreement is expected.

For the filterless and weak filter cases the floating potential is not sensitive to ion mass and the floating potential is close to the same for hydrogen and deuterium. The strong filter case (Fig. 3) shows a lower floating potential for hydrogen than deuterium which reflects a

higher plasma electron temperature for hydrogen and a lower plasma potential.

For a constant source pressure, the floating potential depends on the magnitude of the injected electron current which influences the electron temperature.[10] That is, an increase in arc current results in a more negative floating potential according to equation (1) as shown in Figure 4. The grid potential for the weak filter falls more rapidly than the dependence on electron temperature, probably because of energetic electrons leaking into the extraction region. The question of electron energy flow through the magnetic flux in a source has been described by Holmes[16] who investigated the scaling of primary and bulk electron flow.

Besides source operation indicators of arc voltage, arc current and ion saturation current density, the floating potential of the extraction grid is an good qualitative indicator of the source operating mode and plasma conditions. The data of Fig. 3 and 4 show the influence of the significant parameters such as gas pressure and magnetic flux on the potential of this source element.

C. Efficiency

One concern with the internal filter structure is its influence on the magnitude and uniformity of the extraction current density. The filter rods themselves add anode loss area for primary electrons and the magnetic fields act as a geometric block to ions drifting toward the extraction grid. In addition the axial distribution of the plasma potential in the injection region is flatter so that the drift of ions

into the filter is slower. Measurements of ion flux density in the cusp fields near the bucket wall show that the ion density is not affected by the magnetic flux until ~80 gauss-cm of flux is encountered. Toward the wall, the ion velocity is considered to be thermal (about 0.04 V of energy) so that a full gyrations encloses 60 gauss-cm of magnetic flux. It takes ~ 60 gauss-cm of flux for an electron of 80 V energy to make a full gyration. The ions drifting toward the extraction plane see a potential drop of at least 0.5V and the filter fields of 135 gauss-cm do not impeed the flow of ions. Since the filter fields are designed to reflect energetic electrons back into the injection region, the extraction region lacks the ion production term and only loss terms remain. These are reasons to conclude that the ion flux delivered to the extraction plane for a given injected power is reduced when the filter is added to the source. For example, the standard bucket efficiency is 10 $mA/cm^2/kW$ of arc power. Adding the weak filter reduced the efficiency by ~ 30% to 6.7 $mA/cm^2/kW$ and the strong filter reduced the efficiency by 50% to 5 $mA/cm^2/kW$. If the magnetic fields were to affect the ion flow through the filter plane (the strong filter has 230 gauss-cm of flux) it might be expected that deuterium ions would more easily pass through because of their mass. The observed efficiency difference between the two gases is insignificant. This is inconclusive however because the injection and extraction region plasma potentials are different for the two gases.

Moving the strong filter plane to 9.5 cm from 5.3 cm from the exit electrode caused only about a 10% reduction in efficiency. The additional ion loss area was estimated to be only 10% larger since the major loss area is the extraction grid rather than the side walls.

D. Electron Energy

To measure changes in source plasma properties caused by the addition of the magnetic filter. Langmuir probes were positioned in front of and behind the filter plane. Some detailed measurements were made by positioning a probe axially along the centerline.

The objective of the magnetic filter was to eliminate the energetic electrons from the extraction region and thus reduce the production of molecular ions near the extraction plane. Consistent with eliminating energetic electrons Leung[17] and Holmes[18] have shown that the bulk electron temperature becomes lower as the electrons pass through the filter. A bulk temperature reductions to less than 5 eV is desirable to keep the tail of the distribution from producing an appreciable fraction of molecular ions.[19]

For the filterless bucket, the plasma potential and the electron temperature increased with arc power or with arc current for a constant discharge voltage. With deuterium at 5 mT the electron temperature and the plasma potential at the extraction grid show an increase from 4 to 5.5 eV of electron temperature and an increase from 0.7 to 1.8 volts above anode of plasma potential as the arc power was increased from 15 kW to 30 kW. The installation of the weak filter at 9.5 cm from the extraction grid led to a reduction of the electron temperature from 5.5 eV to 3.7 eV at the extraction grid (0 cm Fig 5). The strong filter shows a greater reduction to about 2 eV.

The installation of the filter not only reduced the electron temperature at the grid but it reduced the energetic tail of the energy distribution function. This is particularly true for the strong filter

where the distribution function is maxwellian over three orders of magnitude (Fig. 6b). By contrast a typical probe electron current energy distribution for the filterless bucket is shown in Fig. 6a. The noted temperature is the bulk electron temperature (lower energy value of the quasi-two slope distribution). The higher energies represent an equivalent temperature of about 15 eV. This distribution is typical everywhere in the filterless bucket. The lower energy component is nearly constant axially whereas each chamber has a different bulk temperatures when the filter is added (Fig. 5). The decrease in electron temperature is consistent with the data of Holmes[18] where the ratio of Te in the extraction chamber to that in the injection chamber is the same for a comparable magnetic flux produced by the weak filter and less for the strong filter.

Across the weak filter (cusp orientation), on the injection side, (Fig. 5) the bulk electron temperature is constant up to about 2.5 cm from the filter plane. There is a monotonic decrease across the filter to 4 eV at about 3.5 cm from the filter plane on the extraction side. This distance represents the position where the magnetic field magnitude is greater than 7.5 gauss. The decrease occurs over about 6 cm. Detailed measurements on the same source but with 6 rods for the filter instead of four, showed a decrease over only 3 cm of axial distance. This corresponds to less field spread in the axial dimension because the rods are closer together.

Operating with hydrogen produces a bulk electron temperature at the grid for the weak filter, slightly higher than operating with deuterium (4.5 eV with H_2, compared with 3.5 eV with D_2). In the source

chamber the temperature is slightly lower for hydrogen. Otherwise the variations have the same form. For the strong filter the temperature in the extraction chamber is again higher for hydrogen; 2.8 eV compared to deuterium at 1.9 eV. The temperature in the injection region is lower for deuterium than for hydrogen; 6 eV compared to 7.5 eV. These differences in electron temperature between hydrogen and deuterium must depend on loss rate differences for ions and electrons which in turn depend on the plasma potential.

E. Plasma Potentials

The plasma potentials in the various parts of the source are related to the energy of the bulk electrons, the ion mass, and to the electron injection rate compared to the relative electron and ion loss rate. For the filterless bucket the plasma potential goes negative near the extraction grid (Figure 7). The addition of the filter rod structure as anode area causes the overall plasma potential to become more positive (Figure 7). Since the filter provides a nearly closed magnetic container for the energetic electrons of the injection region, the plasma potential is fairly flat away from the fields of the filter (note the plasma potential between 13 and 20 cm for the weak filter case; Figure 7). The potential decreases monotonically toward the extraction plane like the filterless bucket with a more or less equivalent drop in plasma potential of about 5 eV ± 0.5 eV.

With hydrogen in the weak filter bucket (Figure 8) the potential drops negative of anode on the extraction side of the filter then levels off. This leveling off may occur because the plasma is close to

maxwellian and since the potential is already negative it will resist ion flow to the side walls. The comparison of Fig. 7 and 8 shows the effect of ion mass. There is an overall decrease in plasma potential for hydrogen for both filter strengths.

F. Ion Flux

The efficiency of ion delivery to the extraction plane is related to ion and electron losses to the walls relative to the production of ions. As already discussed, more arc power is required in the filter source to attain the same extractible current density. The ion flux density in the injection region is increased partly because of the increased power (1.5 times greater in order to have the same output as the filterless source) and partly because of reduced loss area for primaries.

Using the saturated ion flux density and the electron temperature the electron density

$$n_e = \frac{2j_s}{e} \sqrt{\frac{m_i}{kT_e}} \qquad (2)$$

can be estimated. The electron density ratio between the injection region and the extraction grid is 2.7 for the weak filter at the arc power of 35 kW (D_2) and 3.3 for the strong filter. The ion saturation current density ratio between the injection region and extraction grid region increases with increased filter field strength. The ratio is 3.9 for the weak filter and 5.7 for the strong filter whereas for no filter, the usual ratio is about 2. This increased ratio reflects the better confinement of energetic electrons and higher Te in the injection region and the lower electron temperature near the extraction grid. The

stronger gradient of ion flux density at the grid is due to the large loss area of plasma at the grid. (See the hydrogen data, Figure 9).

G. Species

The presence of magnetic field between the region of injected energetic electrons and the region of extracted ions has already been shown to improve the atomic fraction.[7,8,9] The data in Figure 10 compares the filterless bucket with the weak filter and the strong filter as a function of extractible ion current density. The species fraction improvement at 150 mA/cm^2 of extractable current density is 11% for the weak filter and 21% for the strong filter. At lower ion flux density the improvement is even greater. The increase in the atomic fraction came at the expense of decreased D_2^+ and D_3^+ species fractions. The filterless and the filter sources exhibit a similar trend with increasing arc power or extracted current density where the D_2^+ fraction is relatively constant and the D_3^+ ion fraction decreases with additional arc power. The strong filter not only gives a high atomic fraction but over a practical range of operation, 100 to 200 mA/cm^2 of extractible ion current density, the variation is relatively small (about a 4% change). Thus beam energy can be changed without an appreciable change in species.

If the species fractions are compared as a function of arc power, the relative improvement is not so large since the stronger filter requires more arc discharge power. Most of the atomic fraction improvement corresponds to a decrease in the D_2^+ fraction. It might be concluded that the reduction in the D_2^+ fraction at the extraction plane is due to the lack of ionizing electrons in the extraction region.

It is particularly true in rectangular buckets that magnet placement is critical for plasma uniformity. It is easy to have magnetic flux crossing the central, generally field free region, by having some magnets with wrong polarity along any line cusp. This imbalance occurred during one set of experiments with the filterless bucket. Although it is not known how much flux crossed the central region, the data indicated a 7% improvement in the atomic fraction with a corresponding decrease in the D_2^+ and D_3^+ fractions. The presence of this magnetic flux resulted in a decrease of the floating potential of the extraction grid to about 20 volts below anode from a typical value between 30 and 40 volts.

The filter position has relatively little effect on the atomic fraction. One experiment with the strong filter located at 5.5 cm and then at 9.5 cm from the extraction grid indicated about 1% difference. A second experiment compared the weak filter at 9.5 cm from the extraction grid to the same filter at 19.5 cm from the grid by adding an extension of 10 cm to the bucket. In this case the atomic fraction did increase for comparable extractible ion current densities. For the same extraction current density a considerable increase in arc power for the 19.5 cm length was required in order to overcome the increased side wall losses. The increase in the atomic fraction had a corresponding decrease in D_3^+ which is symptomatic of an arc power effect rather than a drift length effect. The same arc power resulted in no difference in the atomic fractions. Thus chamber length is not an effective parameter for species improvement, and a longer chamber only reduces the extractible current density.

The filter rods were oriented in two possible positions; the cusp orientation and the transverse orientation. The transverse arrangement has a slightly higher magnetic flux which returns the energetic electrons back into the source. With the strong magnet filter rods in the 5.5 cm position and with the same arc power (27 kW with jp = 135 mA/cm^2) the transverse orientation resulted in a 1% increase in atomic species with a corresponding reduction in the D_3^+ fraction over the cusp orientation. The slightly higher magnetic flux results in a slightly lower electron temperature at the extraction plane; 1.6 eV compared to 2.1 eV. Likewise the plasma potential is closer to anode; 3 eV compared to about 4 eV for the cusp orientation.

The species fraction dependency on pressure is relatively minor. The optimum pressure for the highest atomic fraction with the strong filter at 30 kW of arc power is between 4 mT and 6 mT. The decrease of the atomic fraction at the higher pressures is due to the production of D_3^+ ions and on the lower pressure side it is due to an increase in the D_2^+ ions. The same basic dependency is observed for the weak filter where the optimum pressure is between 6 mT and 8.5 mT. Previous measurements[9] have indicated that some energetic electrons can leak through the filter by grad-B drift near the side wall fields from the injection chamber into the extraction chamber. Being trapped in the side wall field lines cause these electrons to have longer trajectories than the geometric dimensions. Therefore, only at the lower pressures will the collision mean free path be long enough to allow these drifting energetic electrons to influence conditions in the extraction region resulting in the increase in D_2^+.

H. Plasma Profile

Depending on their configuration square multipole bucket sources can have some undesired magnetic field extending throughout the relatively field free central portion. Although this field is weak the integrated flux through which an electron may travel can be sufficient to deflect it. The square LBL 10 x 10 cm^2 bucket source[10] has a profile asymmetry as shown in Figure 11(a) which can be related to the forward drift of electrons and ions. A rake of four probes covering 7 cm of extraction width is pulled completely across the bucket from wall to wall. The ± 5 cm dimension represents the extent of the extracted ion current. The profile is relatively flat from the north top corner to the south bottom corner with the density falling off toward the other two corners. The variation over the 10 x 7 cm^2 region is ± 15%. When the polarity of the magnetic poles was reversed the flat diagonal density switched to the other two corners. The profile thus depends upon the forward motion of the ions and electrons interacting with the bridging sidewall fields.

The addition of the filter rod magnetic fields improved the uniformity. However, the profile was observed to be arc power dependent since the profile for the cusp oriented filter at 5.3 cm was ± 12% at 35 kW compared to ± 7% at 27 kW. The filter fields are found to influence the profile depending upon the orientation. The cusp orientation flattened the already drooping profile (filterless bucket) on one corner only (Figure 13(b), uniform ± 12%). If the filter rods were rotated 180° to change the magnetic pole polarity, the opposite corner became flatter. The transverse orientation made either the top or bottom fall off in density depending on the field direction.

The forward drift of plasmas ions and primary electrons gyrate on the filter fields causing them to deflect in opposite directions. The primary electrons will be turned back into the source region and the ions drift through the filter plane. The above changes in the extraction plane profile appear to be dependent upon ion deflection rather than upon electron deflection. The main consideration is that the filter fields do affect the profile and thus the filter position relative to the extraction plane can be important. For example at 35 kW of arc power the profile for the cusp orientation at 5.3 cm varies ± 12% and at 9.6 cm the variation is ± 7%. These profile modification effects need further investigation since the filterless bucket already had a poor profile.

I. Power Loading

The rod structure which produces the filter magnetic flux in the source creates a problem when operating the source with the accelerator. The few percent of back-streaming electron power compared to the beam power can be significant in terms of power loading on the rods carrying the magnets. The design incorporates water cooling passages in the space between the square magnet and the cylindrical tube. The cooling capacity permits an overall heat flux of 100 W/cm^2 on the surface. The rods were located so that their centerlines were hidden directly behind an extraction grid structure (Figure 14). Thus only the edge of the rod could intercept direct loading from the back-streaming electrons.

To test the power loading capacity of these rods, the filter source was operated on a beam line. The power loading on the rods was checked by calorimetric measurements. First, the power loading on the filter

rods, due to the arc discharge and filament radiation was measured. The center two rods received the greatest loading by more than a factor of 2. The quasi-steady state temperature of the water was reached in 1.5 sec. More than half of the absorbed power came from the arc and about half was due to the backstreaming electrons. The relative loading depended upon the gas flow and the beam power. The peak loading conditions were with an arc power of 41 kW which produced an extractable ion flux of 180 mA/cm^2 for the strong filter bucket configuration. The gas flow was 4.2 Tl/s and the acclerator power, 590 kW (85 kV and 6.9 Amps). The two central rods received 3.2 kW of beam power loading and the outer two rods received 0.8 kW of beam power. Since the outer rods, which are not in line with direct back-streaming electrons (Fig. 14), receive power from the back-streaming electrons it must have been indirect. Assuming that this indirect loading is uniform over the source cross-section, an estimate can be made of the direct power loading on the central rods. The area of the rod which can be directly hit is known and thus the direct power loading was estimated to be 470 W/cm^2. Although this direct power density loading on the rods was larger than the permitted average it is local and no damage was observed. Also the rod surface at the edge is at an acute angle to the beam back-streaming electrons and thus the power density is reduced.

III. RODLESS FILTER SOURCE

To cite another example of the effect of bridging flux in a source, summary data is discussed which was obtained from a large multipole ion source (10 x 40 cm^2 extraction area).[20] This source had a

backplate with magnets which could be removed to eliminate the bridging fields across the filaments. When the backplate magnets were installed, flux bridging to the side wall magnets covered the filament region. This resulted in an increase of the atomic fraction of 12% from about 73 to 85%. The change in grid potential was from 29 to 15V below anode. The plasma profile with no backplate magnets was flat over the 10 x 40 cm^2 region to ± 5.5% and with the back plate magnets the profile was flat to ± 5%. Thus the changes between backplate magnets and none had little effect on the profile while significantly changing the atomic fraction. With these bridging fields close to the injection region and far from the extraction region may have reduced the influence on the profile. The advantage of this type of magnetic filter system, if its effect could be predictable, is the bridging flux does not require an internal structure. The application of magnet multipoles on the back plate was expected to reduce the loss area for primary electrons and increase the efficiency. Surprisingly there was a slight increase in efficiency. It is thus encouraging that a filter system in a multipole source can indeed provide the species improvement but perhaps not be too costly in terms of efficiency or profile.

IV. SUMMARY

The filter concept has been shown capable of an atomic species improvement of at least 10% from the filterless bucket atomic species fraction. Evidence is cited in this paper that it is not strictly necessary to have a rod structure carrying permanent magnets mounted inside the source in order to attain the same goal. It suffices only to

have flux between the electron injection region and the region of extraction. It is probable that many multipole sources may unintensionally have some magnetic flux which crosses between the filament and the extraction region. The benefit of the filter plane as described herein is that the position and quantity of bridging flux is known. This data provides the basis on which a source can be designed to produce a desired atomic species. Some indications were observed that the magnetic flux affects ion drift which influences the profile. The position of the filter close to the grid produced a slightly higher atomic fraction but for good profile it needs to be further away from the grid.

REFERENCES

1. W. L. Bardner, G. C. Barber, C. W. Blue, W. K. Dagenhart, H. H. Haselton, J. Kim, M. M. Menon, N. S. Ponte, P. M. Ryan, D. E. Schechter, W. L. Stirling, C. C. Tsai, J. H. Whealton, and R. E. Wright, Rev. Sci. Instrum. 53, 424, 1982.

2. A. P. H. Goede and J. S. Green, Proceedings of 8th Symposium on Engineering Problems of Fusion Research, San Francisco, 680 (1979).

3. Y. Arakawa, M. Akiba, M. Araki, H. Horizke, T. Itoh, M. Kawai, M. Kuriyama, S. Matsuda, M. Matsusha, V. Mizutani, T. Ohga, Y. Ohara, Y. Okumura, J. Sakuraba, T. Shibata, H. Shirakata, and S. Tanaba, Japan Atomic Energy Research Institute JAERI-M 8869 (1980).

4. K. H. Berkner, C. F. Burrell, V. L. Jacobson, A. F. Lietzke, Bull. Am. Phys. Soc. 27, 1136 (1982).

5. T. Obiki, A. Sasaki, F. Sano and K. Vo, Rev. Sci. Instrum. 52 1445 (1981).

6. H. Horike, M. Akiba, Y. Arakawa, S. Matsuda, and J. Sakuraba, Rev. Scie. Instrum. 52, 567, (1981).

7. K. W. Ehlers and K. N. Leung, Rev. Sci. Instrum. 52, 1452, (1981).

8. K. W. Ehlers and K. N. Leung, Rev. Sci. Instrum. 53 1423 (1982).

9. P. A. Pincosy, K. N. Ehlers, Proceedings of the Third Neutral Beam Workshop, Gatlinburg, TN, 1981.

10. K. W. Ehlers and K. N. Leung, Rev. Sci. Instrum. 50, 1353 (1979).

11. A. F. Lietzke, Bull. Amer. Phys. Soc. 27 1057, (1982).

12. K. W. Ehlers and K. N. Leung, Rev. Sci. Instrum. 54, 1296 (1983)

13. K. H. Berkner, W. S. Cooper, J. H. Feist, D. J. Massoletti, H. M. Owren, J. A. Paterson, and R. P. Wells, Bull. Amer. Phys. Soc., 982, (1980).

14. D. Goebel, Phys. Fluids, 25, 1093, (1982).

15. K. Yamamoto, T. Okuda, J. Phys. Soc., Japan 11, 57, (1956).

16. A. J. T. Holmes, Rev. Sci. Instrum. 53 1517, (1982).

17. K. N. Leung, K. W. Ehlers and M. Bacal, Rev. Sci. Instrum., 54, 56, 1983.

18. A. J. T. Holmes, Rev. Sci. Instrum, 53 1523, (1982).

19. C. F. Chan, C. F. Burrell, and W. S. Cooper, J. Appl. Phys. 54 6119, (1983).

20. P. A. Pincosy, K. H. Ehlers, A. F. Lietzke, H. M. Owren, J. A. Paterson, and M. C. Vella, LBL-17604 (1984)

Figures

Figure 1: 10 x 10 cm^2 extraction area LBL multi-pole field bucket source. Filter rods provide transverse magnitic flux.

Figure 2: Magnetic field distribution midway between filter rods along centerline (strong filter).

Figure 3: Grid floating potential dependence on source pressure

1) strong filter: P_{arc} = 30 kW

   a) deuterium □
   b) hydrogen ▲

2) weak filter: P_{arc} = 33 kW, deuterium ◆

3) filterless: P_{arc} = 20 kW, hydrogen ▼, deuterium ◇

Figure 4: Grid floating potential dependence on arc current: source pressure 5mT

1) strong filter

   a) deuterium □
   b) hydrogen ▲

2) weak filter ◆

Figure 5: Axial variation of source bulk electron temperature: weak filter deuterium; 35kW arc power: 5 mT source pressure. Filter position at 9.5 cm.

1) hydrogen □

2) deuterium ▲

Figure 6: Electron energy distribution at the grid:

1) Filterless: grid potential = -23V
   P_{arc} = 22 kW
   T_e = 5.2 eV

2) Strong filter: grid potential = -3.6V
   P_{arc} = 26 kW
   T_e = 1.6 eV

Probe bias with respect to grid potential

Figures (Continued)

Figure 7: Axial variation of the plasma potential for deuterium

1) strong filter: P_{arc} = 29 kW ◆
2) weak filter: P_{arc} = 35 kW ▲
3) filterless: P_{arc} = 23 kW □

} source pressure 5mT

Figure 8: Axial variation of the plasma potential for hydrogen at source pressure 5 mT

1) weak filter: P_{arc} = 35 kW ▲
2) strong filter: P_{arc} = 35kW □

Figure 9: Axial variation of ion flux density for the weak filter: P_{arc} = 35kW

1) deuterium □
2) hydrogen ▲

Figure 10: Species variation with extractible ion current density

1) strong filter □
2) weak filter ▲
3) filterless ◆

Figure 11: Plasma Profile at extractible current density of 200 mA/cm^2

1) filterless: source pressure 5.5 mT deuterium and P_{arc} = 22 kW, j_p = 200 mA/cm^2
2) strong filter: source pressure 5.5 mT deuterium and P_{arc} = 37 kW, j_p = 200 mA/cm^2

Figure 12: Schematic of backstreaming electron impingment on the filter rods

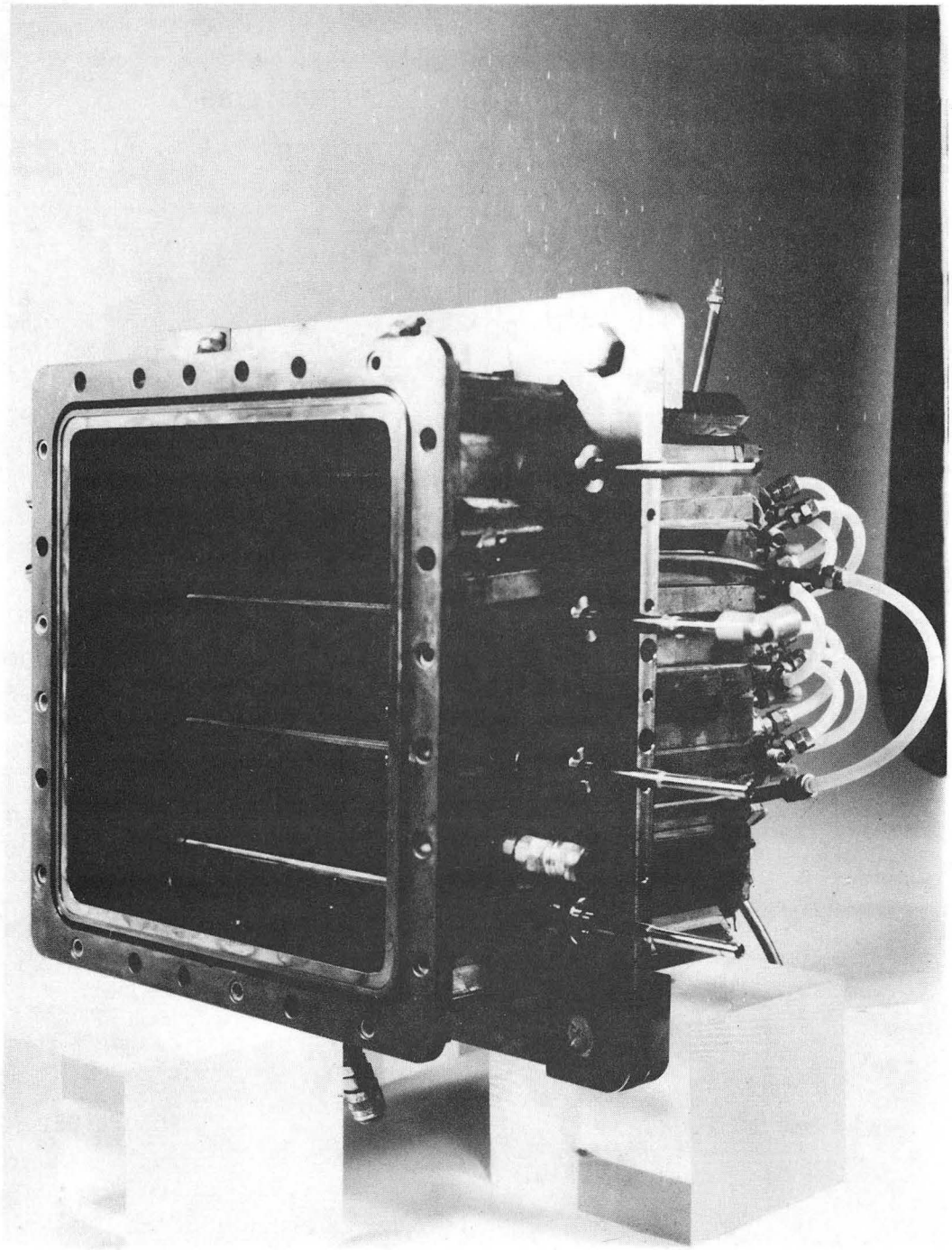

Fig. 1 CBB 818-7450

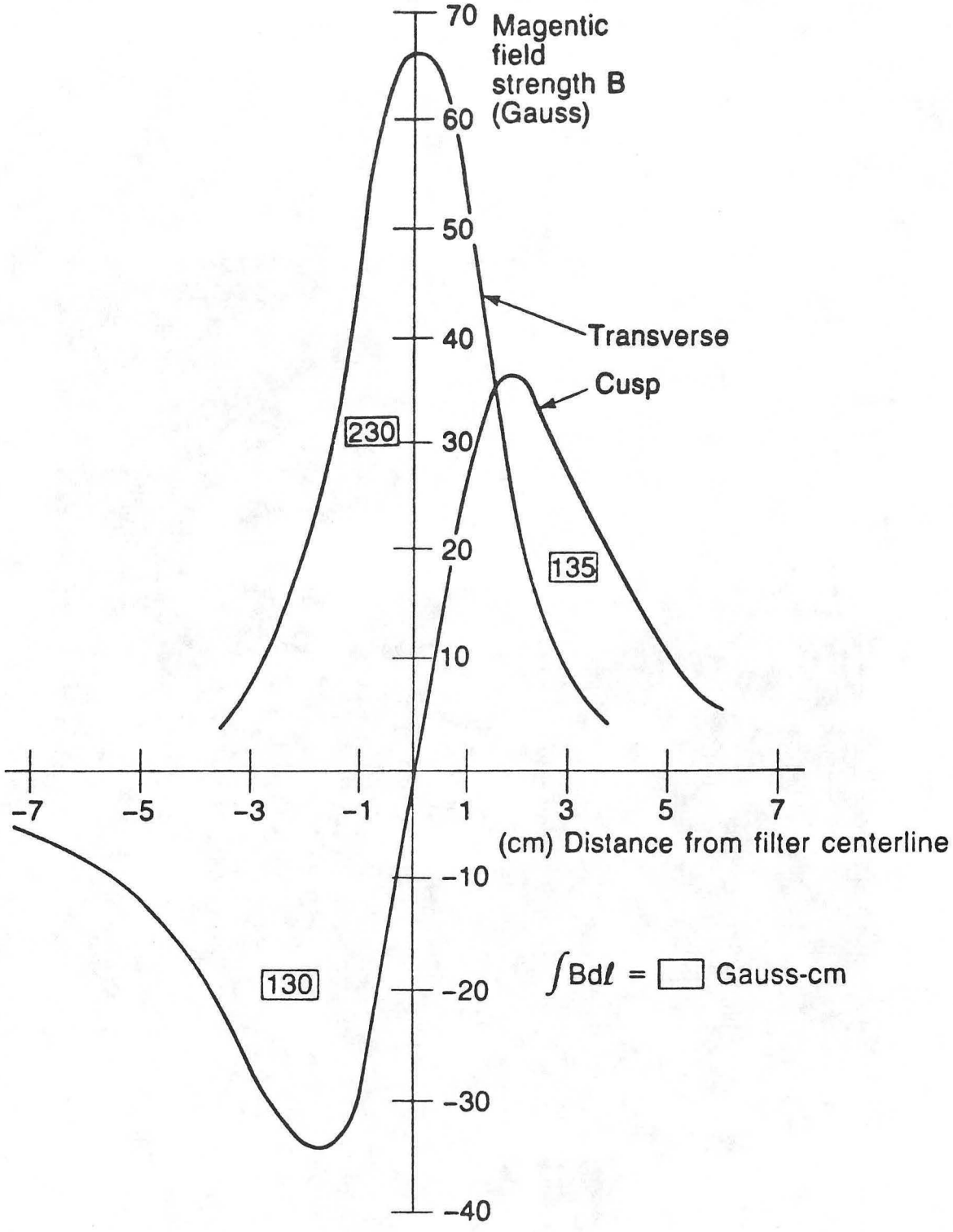

XBL 851-6934

Fig. 2

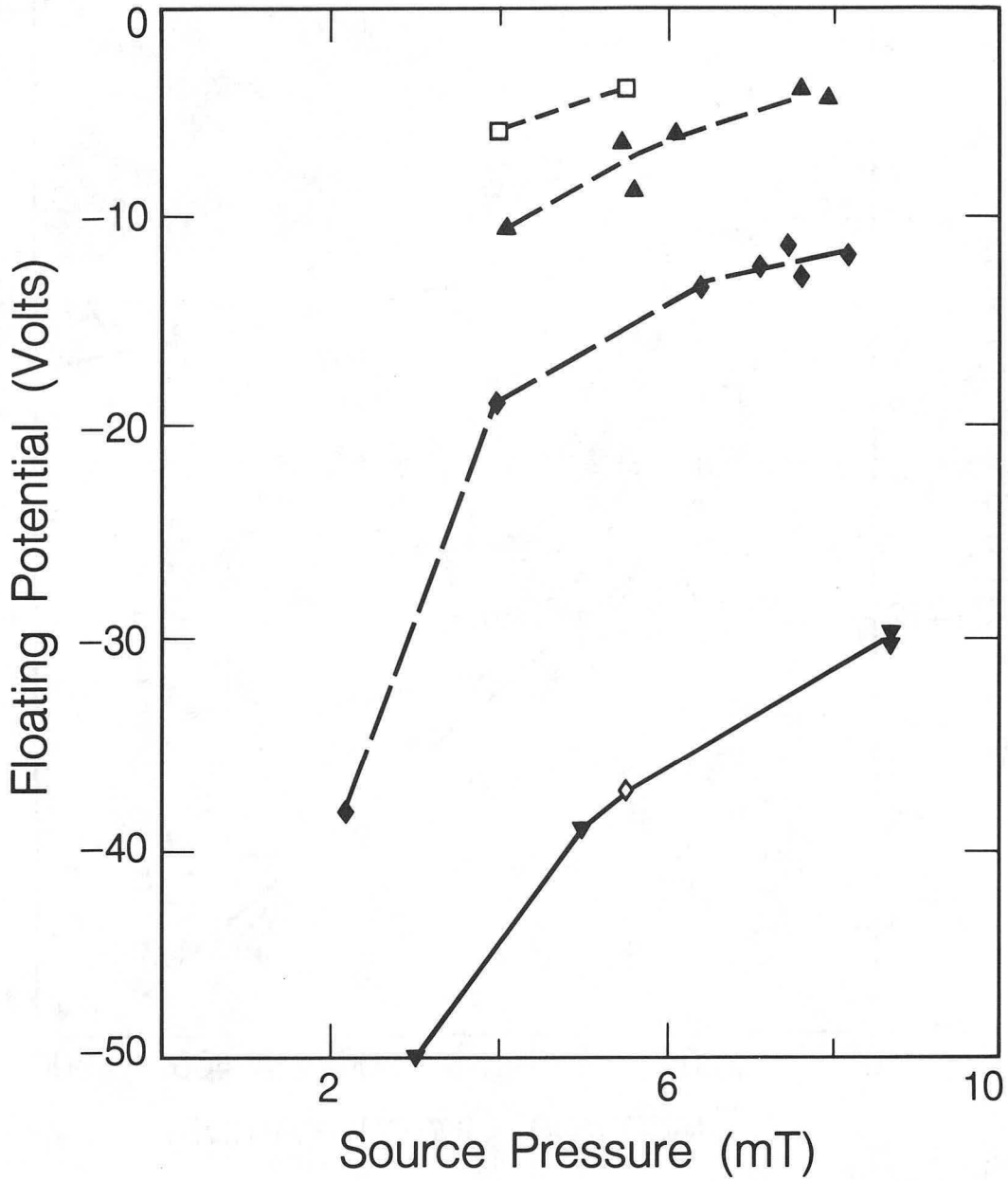

XBL 852-9737

Fig. 3

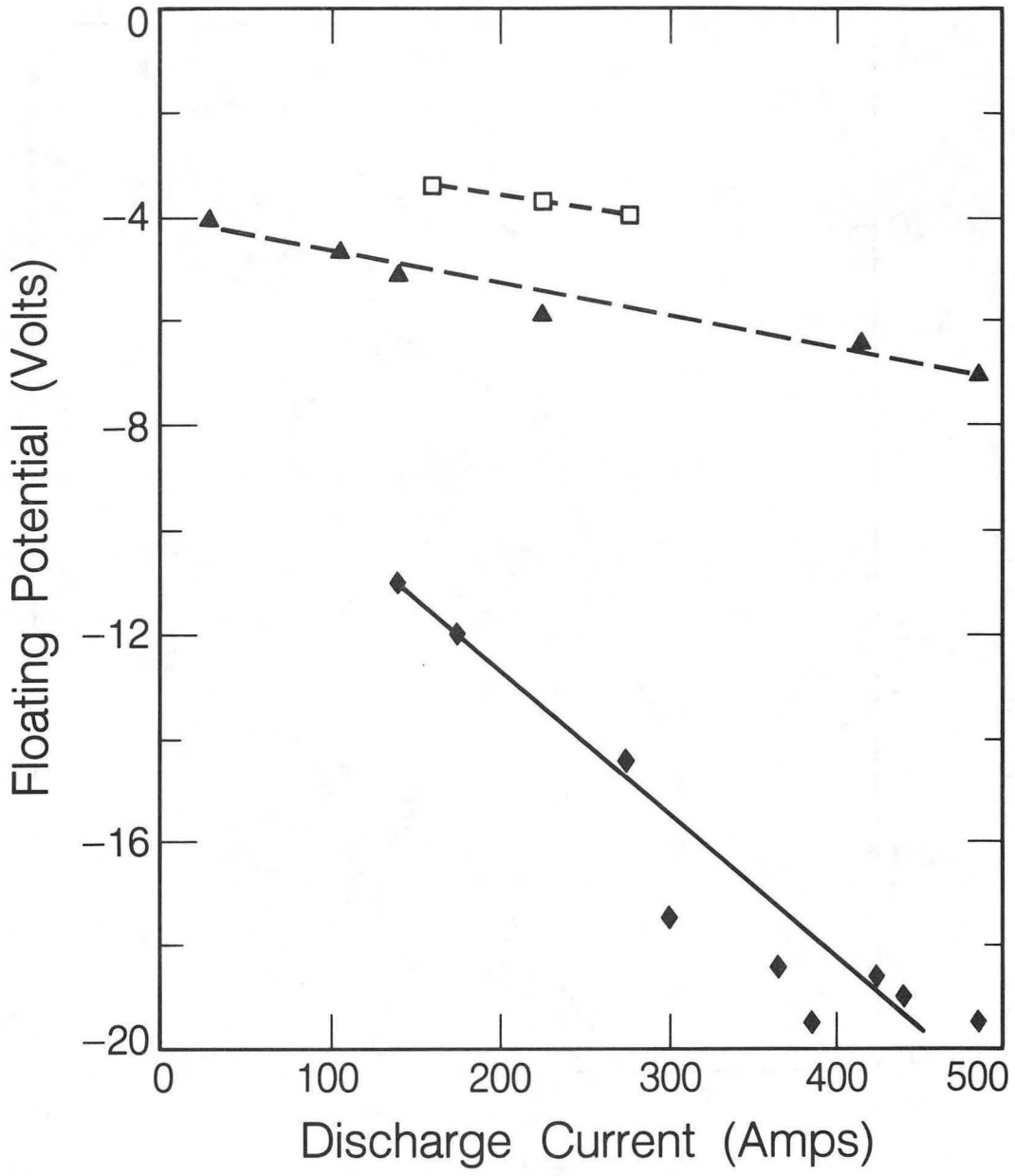

XBL 852-9747

Fig. 4

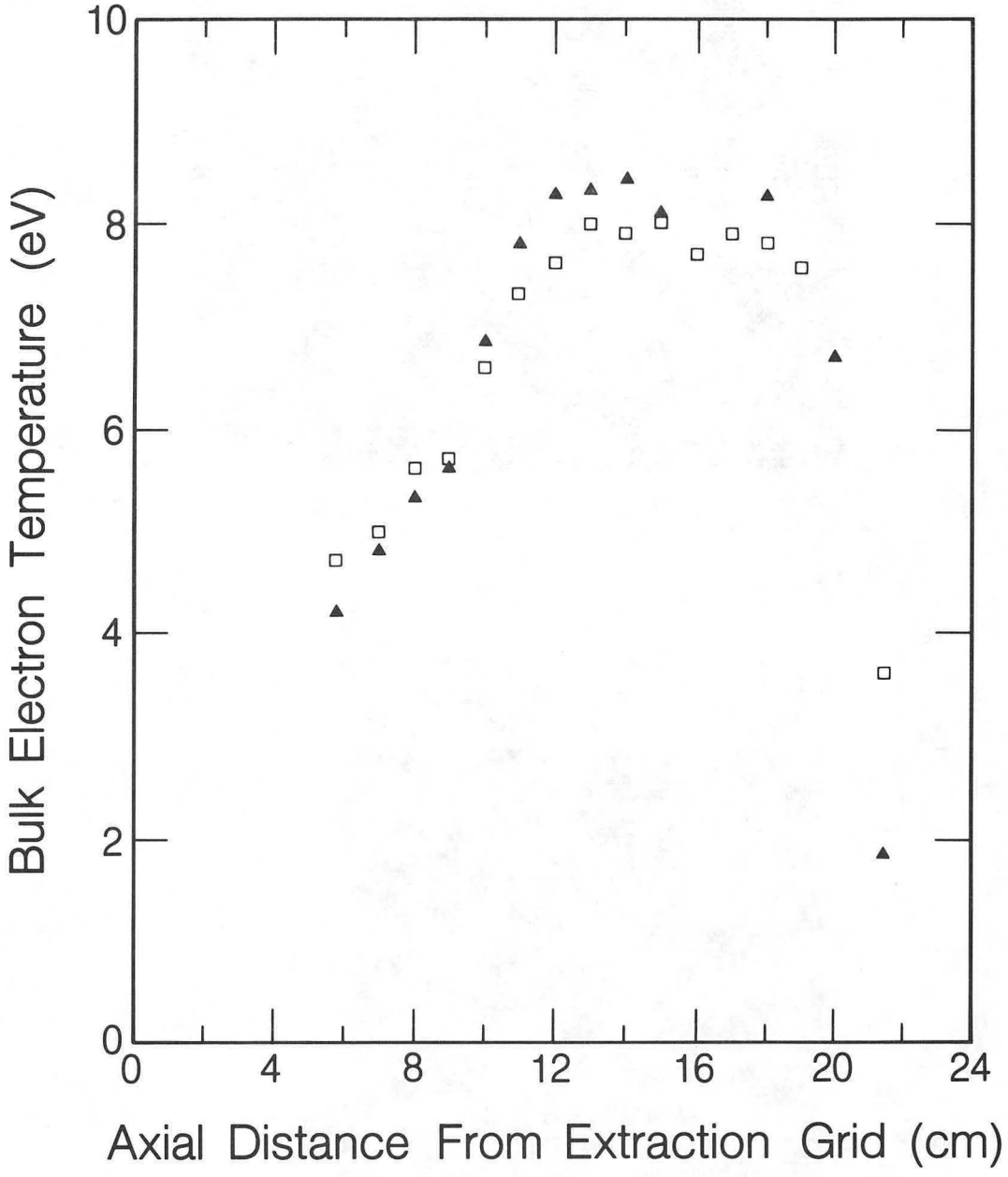

XBL 852-9738

Fig. 5

Fig. 6

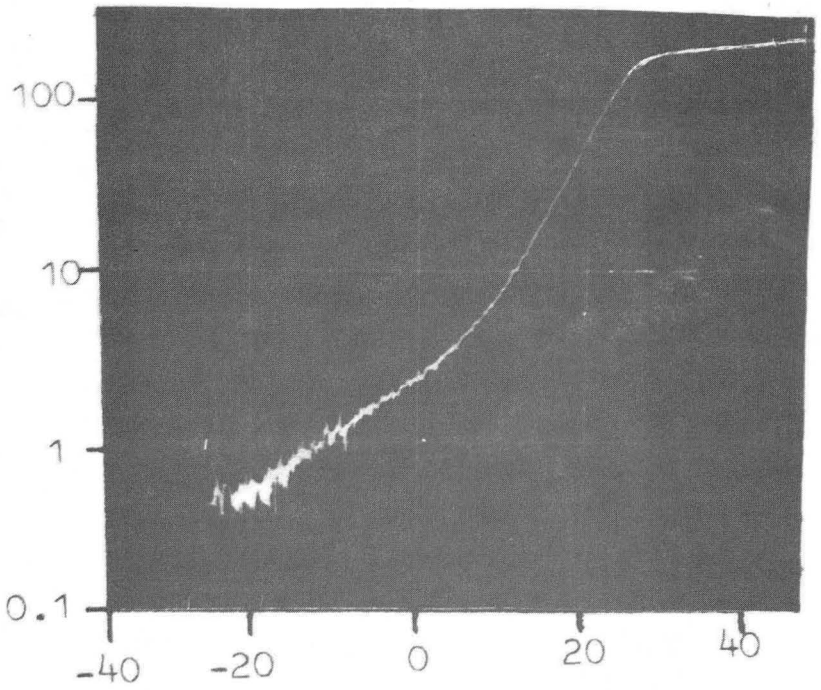

Bias Voltage

Filterless

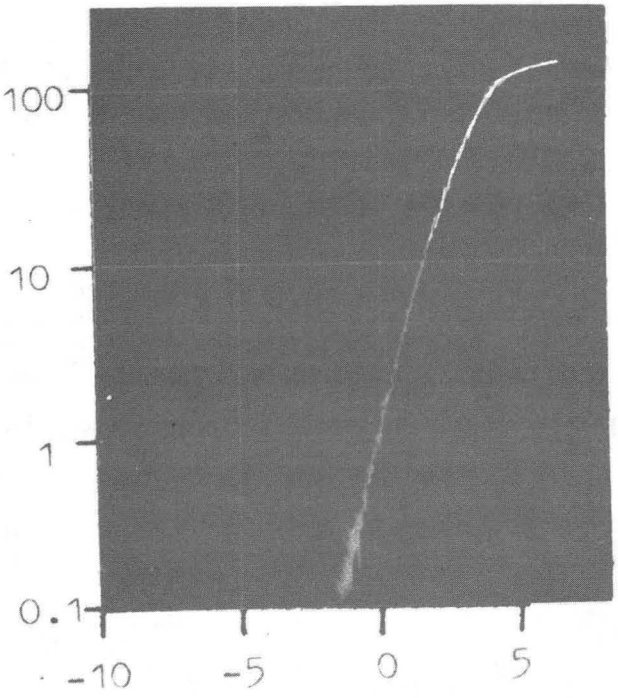

Bias Voltage

XBB 851-503

Strong Filter

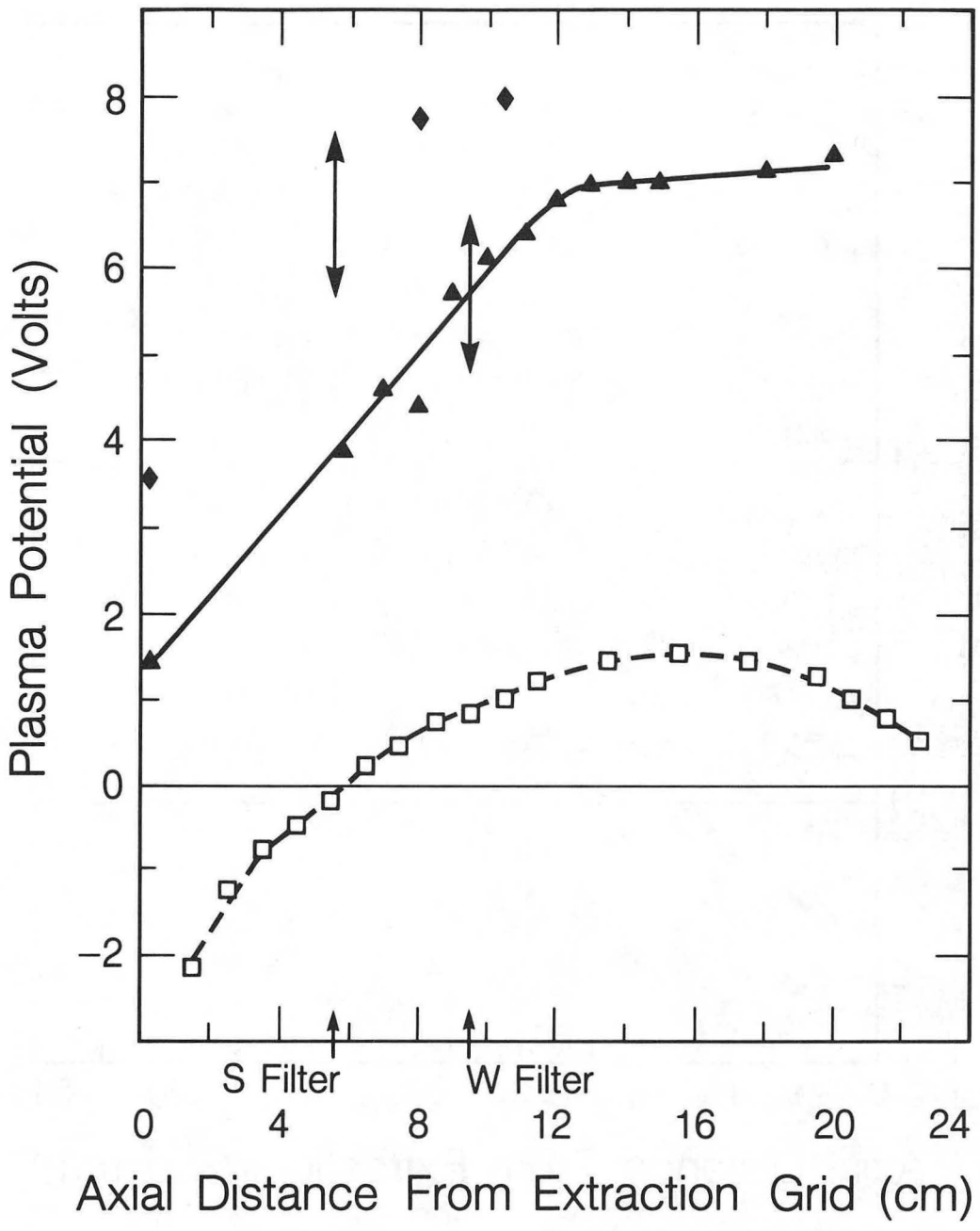
Plasma Potential (Volts)
8
6
4
2
0
−2
S Filter
W Filter
0
4
8
12
16
20
24
Axial Distance From Extraction Grid (cm)
XBL 852-9740

Fig. 7

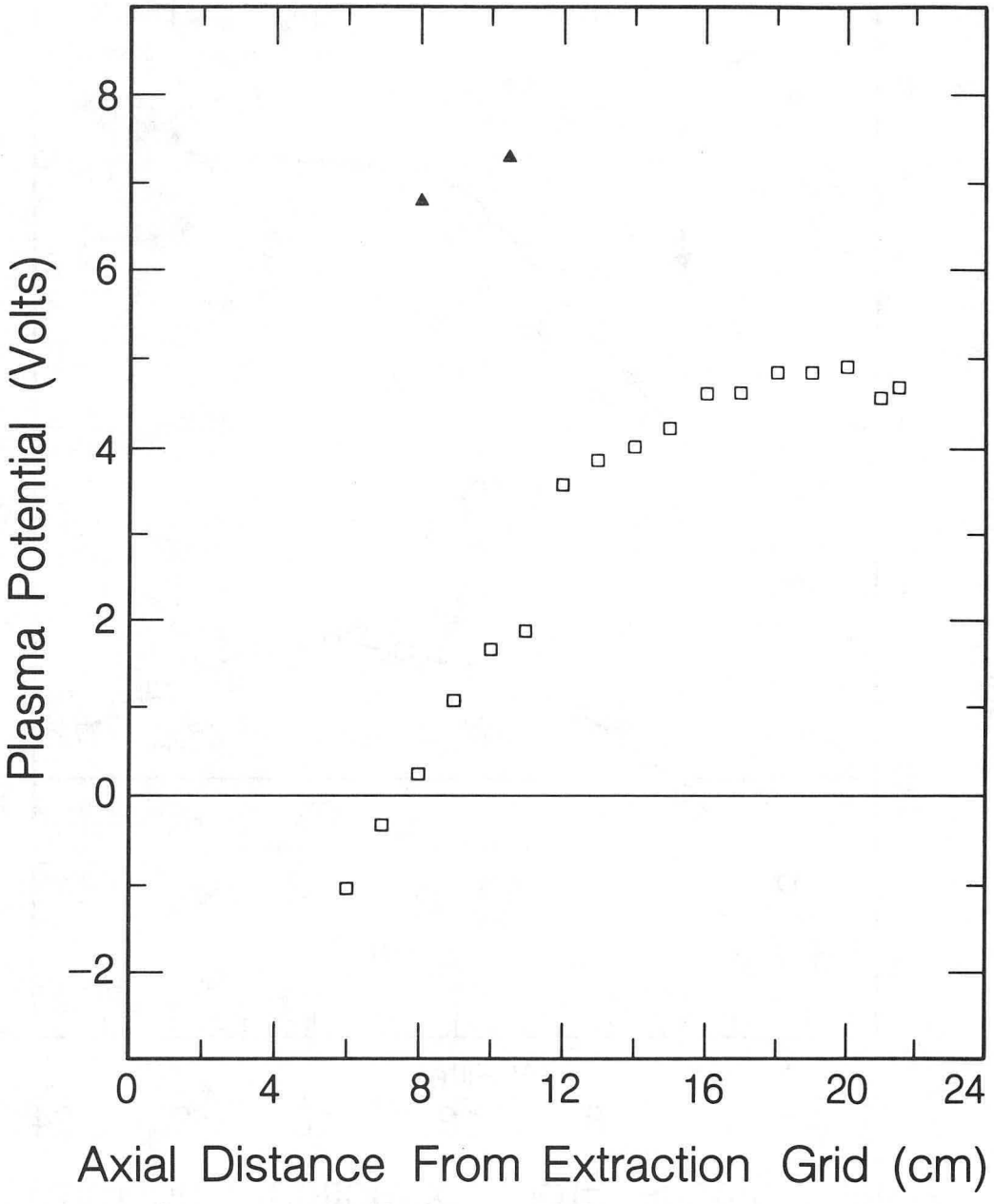

XBL 852-9739

Fig. 8

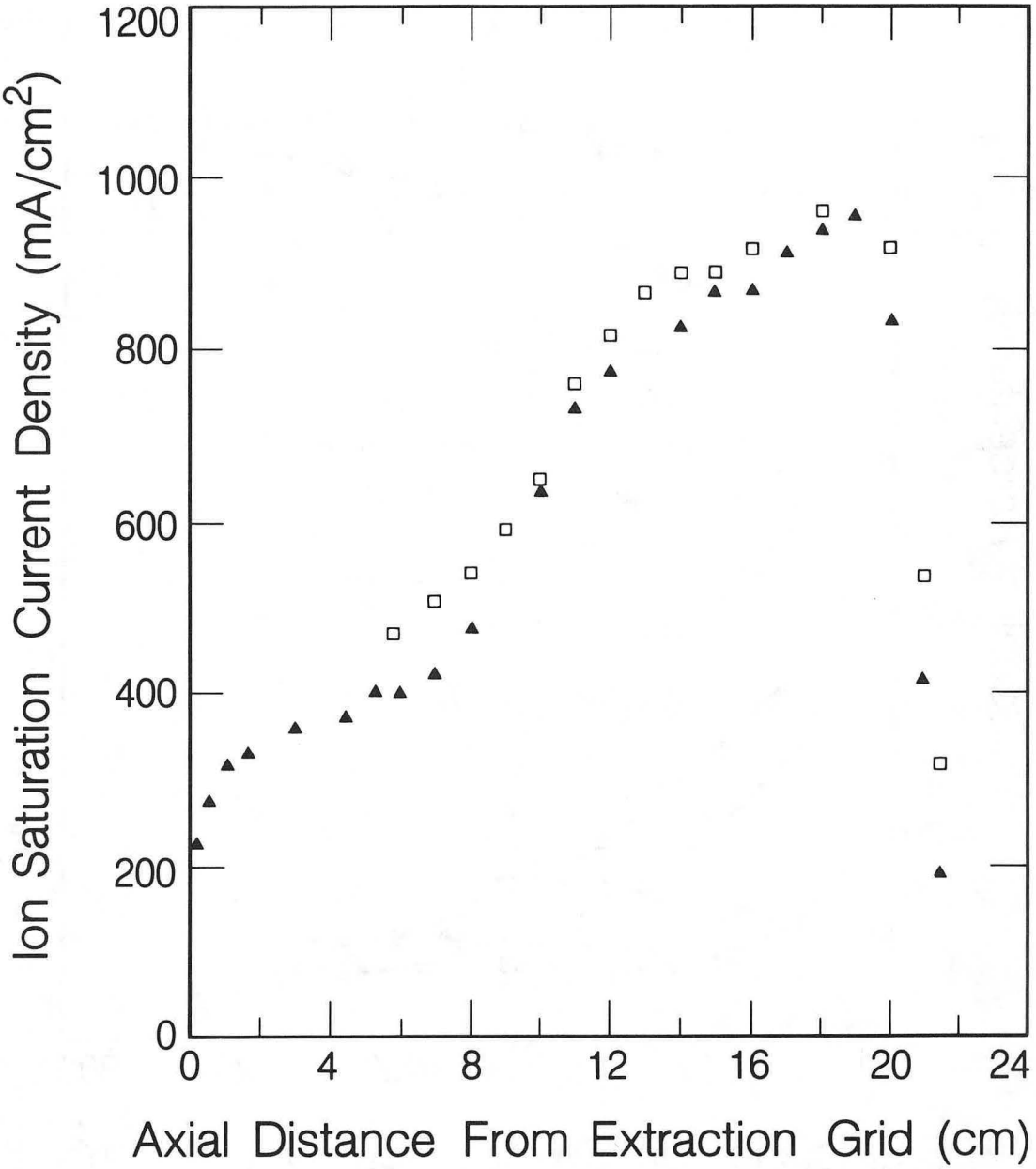

XBL 852-9744

Fig. 9

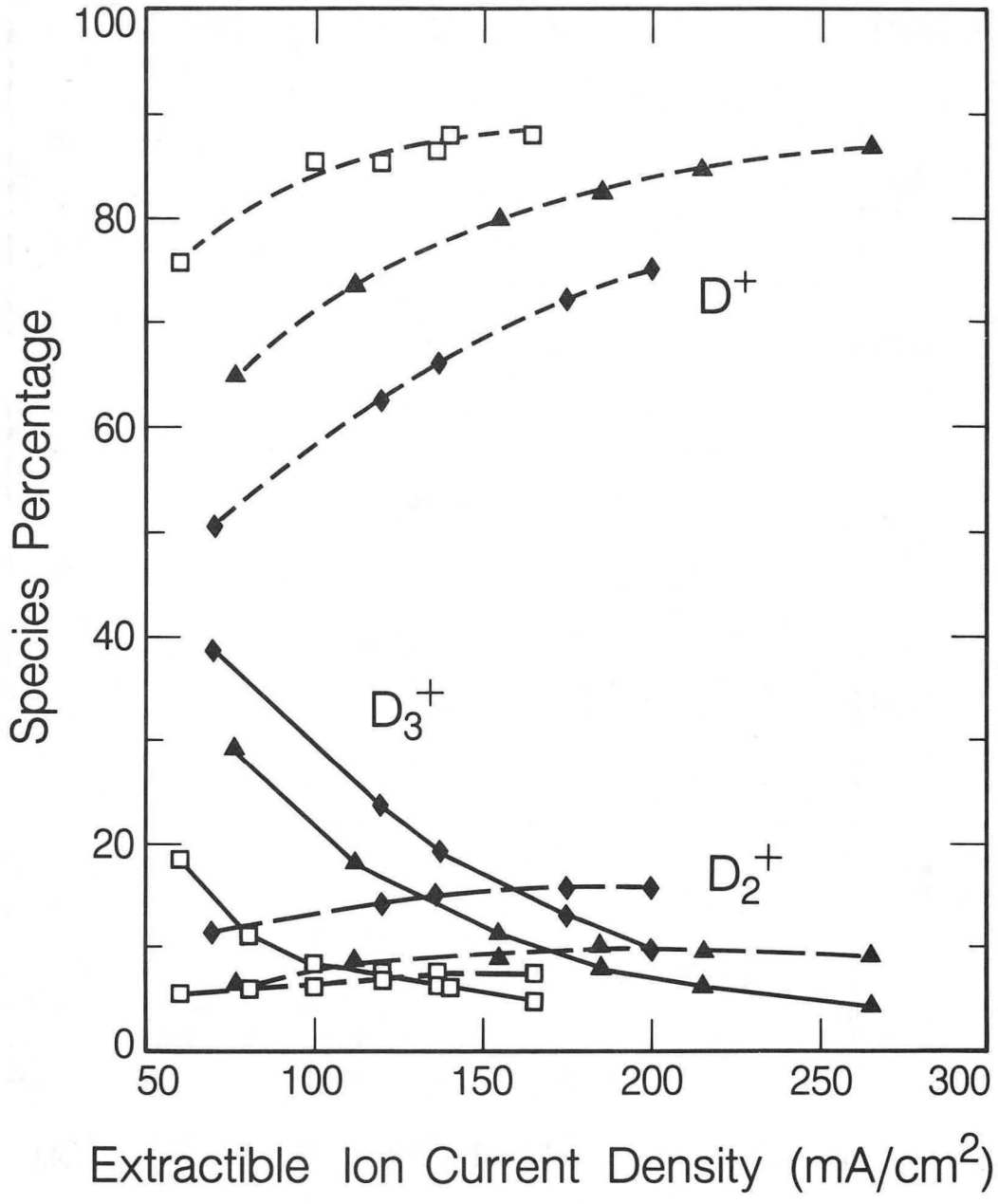

XBL 852-9748

Fig. 10

Fig. 11

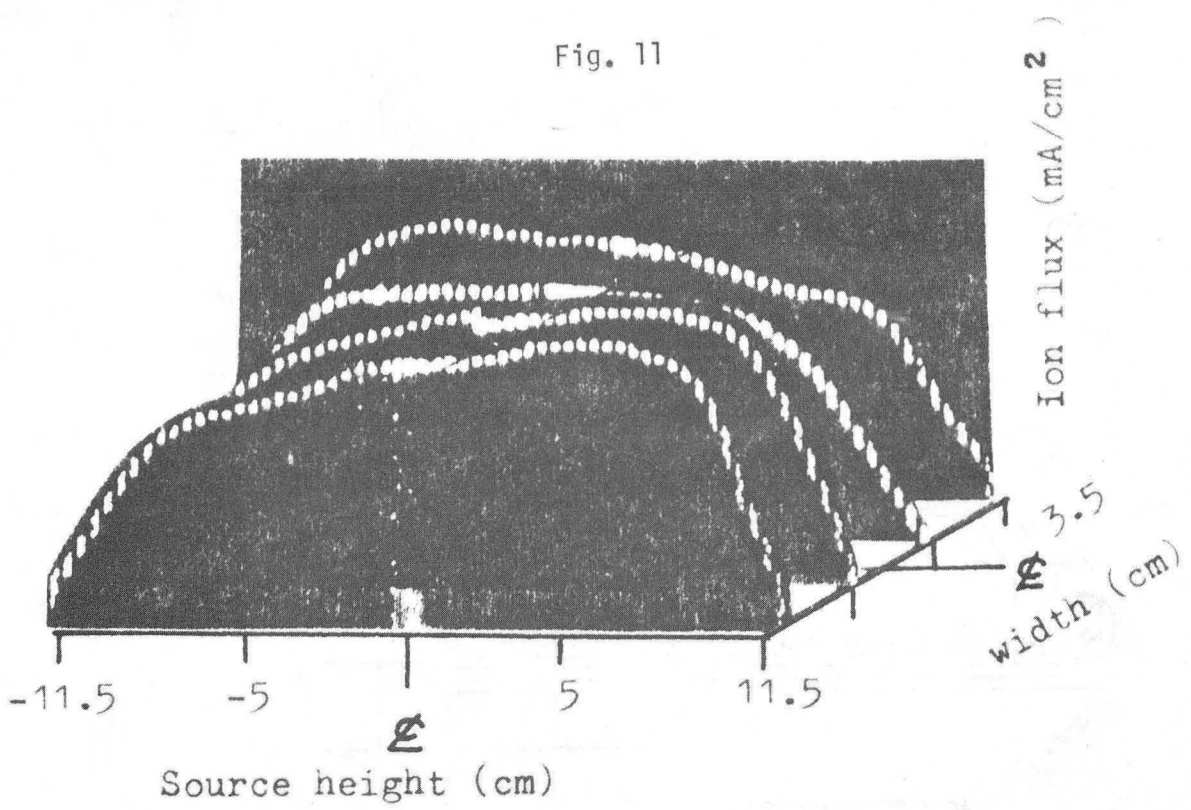

(a) Filterless

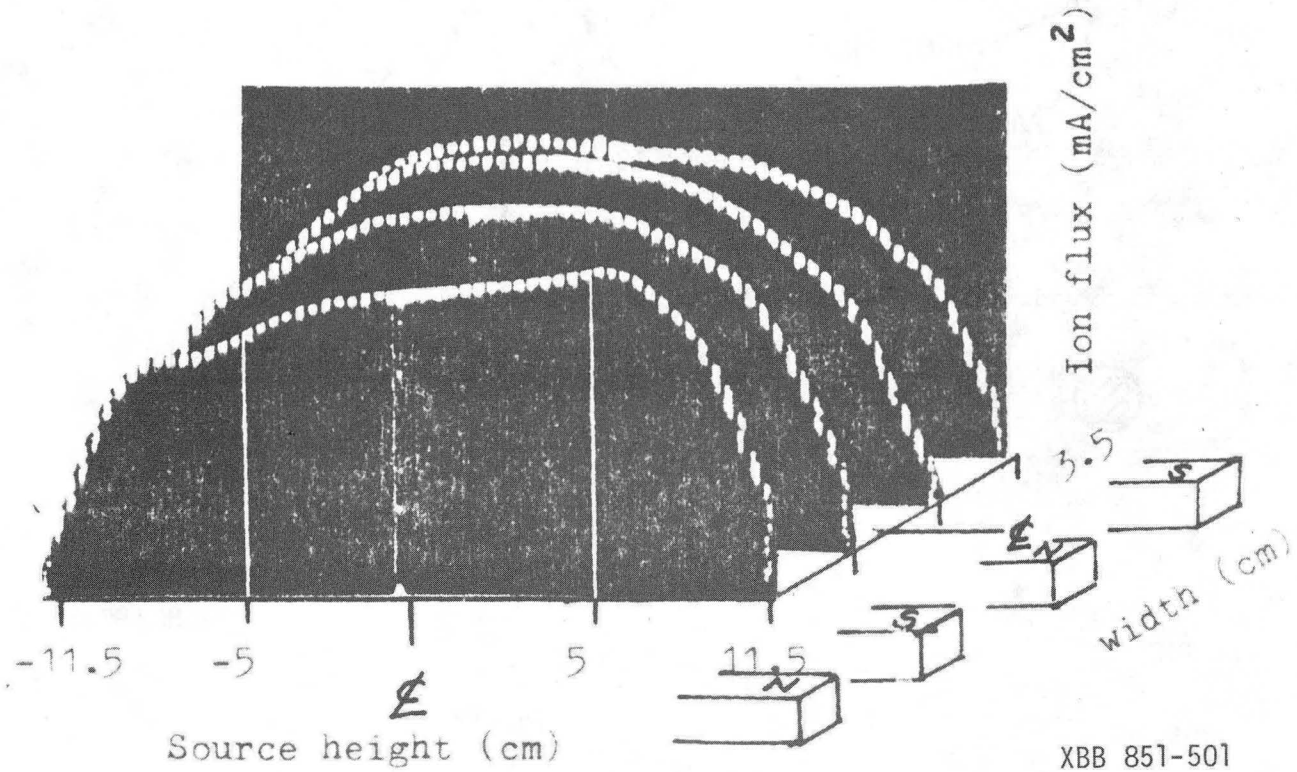

XBB 851-501

(b) Strong Filter

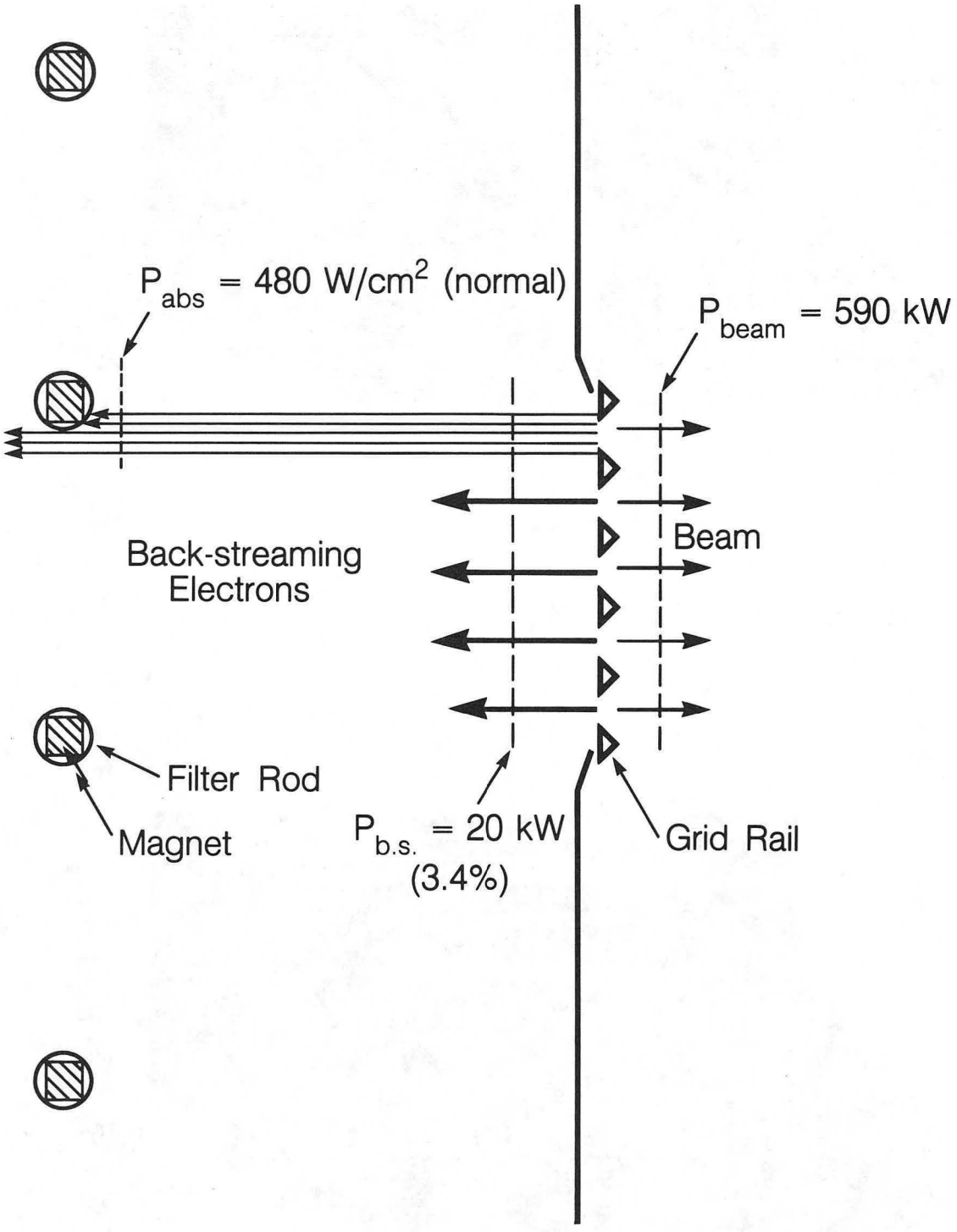

XBL 852-9736

Fig. 12

LAWRENCE BERKELEY LABORATORY
TECHNICAL INFORMATION DEPARTMENT
UNIVERSITY OF CALIFORNIA
BERKELEY, CALIFORNIA 94720